Detection of Human βV-Tubulin Expression in Epithelial Cancer Cell Lines by Tubulin Proteomics†

Pascal Verdier-Pinard,‡,§,|| Shohreh Shahabi,§,|| Fang Wang,⊥ Berta Burd,‡ Hui Xiao,‡ Gary L. Goldberg,§ George A. Orr,‡ and Susan Band Horwitz*,‡

Department of Molecular Pharmacology, Department of Obstetrics and Gynecology and Women's Health, Division of Gynecological Oncology, and Laboratory for Macromolecular Analysis and Proteomics, Albert Einstein College of Medicine, Bronx, New York 10461

Received May 27, 2005; Revised Manuscript Received October 7, 2005

ABSTRACT: Tubulin, the constitutive protein of microtubules, is a heterodimeric protein with an α and β subunit, encoded in vertebrates by six and seven different genes, respectively. Each tubulin isotype can be identified by its divergent C-terminal sequence. Nevertheless, two groups of β-tubulin isotypes can be distinguished by sequence alignment; one includes βI-, βII-, βIVa-, and βIVb-tubulin, and the other includes βIII-, βV-, and βVI-tubulin. βIII-tubulin overexpression has been associated with microtubule destabilization and resistance to Taxol. Recent data indicate that mouse βV-tubulin overexpression in CHO cells results in profound microtubule disorganization and dependence of cells on Taxol for growth. Mouse and human βV-tubulin sequences display several differences, such as their respective extreme C-terminus, suggesting that they may have different effects on microtubule stability and different affinities for drugs. When high-resolution isoelectric focusing, in-gel CNBr cleavage, and mass spectrometry were combined, we detected for the first time the βV-tubulin protein in human cell lines and found that it was highly expressed in Hey, an epithelial ovarian cancer cell line. Our data confirm that human and rodent βV-tubulins are distinct and indicate that, regardless of species, βIII- and βV-tubulin may be expressed in a complementary pattern at the protein level. Therefore, both βIII- and βV-tubulin expression levels should be systematically determined to assess the role of differential tubulin isotype expression in the response of tumors to drugs targeting microtubules.

Microtubules are dynamic polymers of tubulin that are involved in several cellular processes, including cell division. Tubulin is a heterodimeric protein made of α and β subunits, encoded in vertebrates by six and seven different genes, respectively. Microtubule dynamics is defined by the stochastic transition between phases of growth and shrinkage that may be regulated by the β-tubulin isotype composition (*1*). Each tubulin isotype is highly homologous across species, differing from other isotypes mostly by the last 15 amino acids. These divergent C-terminal sequences are the site of numerous post-translational modifications, such as glutamylation, and are involved in the binding of microtubule-associated proteins (MAPs)[1] and motors (*2*).

β-Tubulin isotypes can be classified into two divergent groups of sequences: (1) βI-, βII-, and βIV-tubulin and (2) βIII-, βV-, and βVI-tubulin (Figure 1). Except for their C-termini, βIII- and βV-tubulin sequences are closely related. The expression of specific tubulin isotypes in tissues strongly suggests that the existence of multiple tubulin isoforms has a physiological role (*2*). βIII-Tubulin is expressed specifically in neuronal tissues and in testis, whereas βVI-tubulin has been detected only in the microtubule marginal band of bird erythrocytes and mammalian platelets, where it is present as the only β-tubulin (*2*). βIII-Tubulin has also been detected in numerous cancer cell lines and tumors of different histological origin (*3*). Chicken βV-and βIII-tubulins have a complementary pattern of expression, as determined by RT-PCR, with βV-tubulin being expressed ubiquitously except in the brain and βIII-tubulin being expressed only in the brain (*4*).

βIII-Tubulin has distinct assembly properties compared to βII-, βIV-, or unfractionated tubulin. βIII-Tubulin required the highest critical concentration of tubulin for assembly, exhibited a distinct delay in nucleation, and proceeded to polymerize at a slower rate compared to other isotypes (*5*).

† This work was supported in part by National Cancer Institute Grants CA083185 and CA077263, National Foundation for Cancer Research, and American Cancer Society Grant ROG-03-253-01 (to S.B.H.).

* To whom correspondence should be addressed. Telephone: (718) 430-2163. Fax: (718) 430-8959. E-mail: shorwitz@aecom.yu.edu.

‡ Department of Molecular Pharmacology.

§ Department of Obstetrics and Gynecology and Women's Health, Division of Gynecological Oncology.

|| These two authors contributed equally to this work.

⊥ Laboratory for Macromolecular Analysis and Proteomics.

[1] Abbreviations: MAPs, microtubule-associated proteins; RT-PCR, reverse transcriptase−polymerase chain reaction; SDS−PAGE, sodium dodecyl sulfate−polyacrylamide gel electrophoresis; PBS, phosphate-buffered saline; FBS, fetal bovine serum; DTT, dithiothreitol; IPG, immobilized pH gradient; IEF, isoelectric focusing; HRP, horseradish peroxidase; ECL, enhanced chemoluminescence; MALDI−TOF MS, matrix-assisted laser desorption ionization−time-of-flight mass spectrometry; MS/MS, tandem mass spectrometry; LC/ESI MS, liquid chromatography coupled to electrospray ionization mass spectrometry; 2D, second dimension; pI, isoelectric point; SILAC, stable isotope labeling with an amino acid in culture.

10.1021/bi051004p CCC: $30.25
Published on Web 11/08/2005

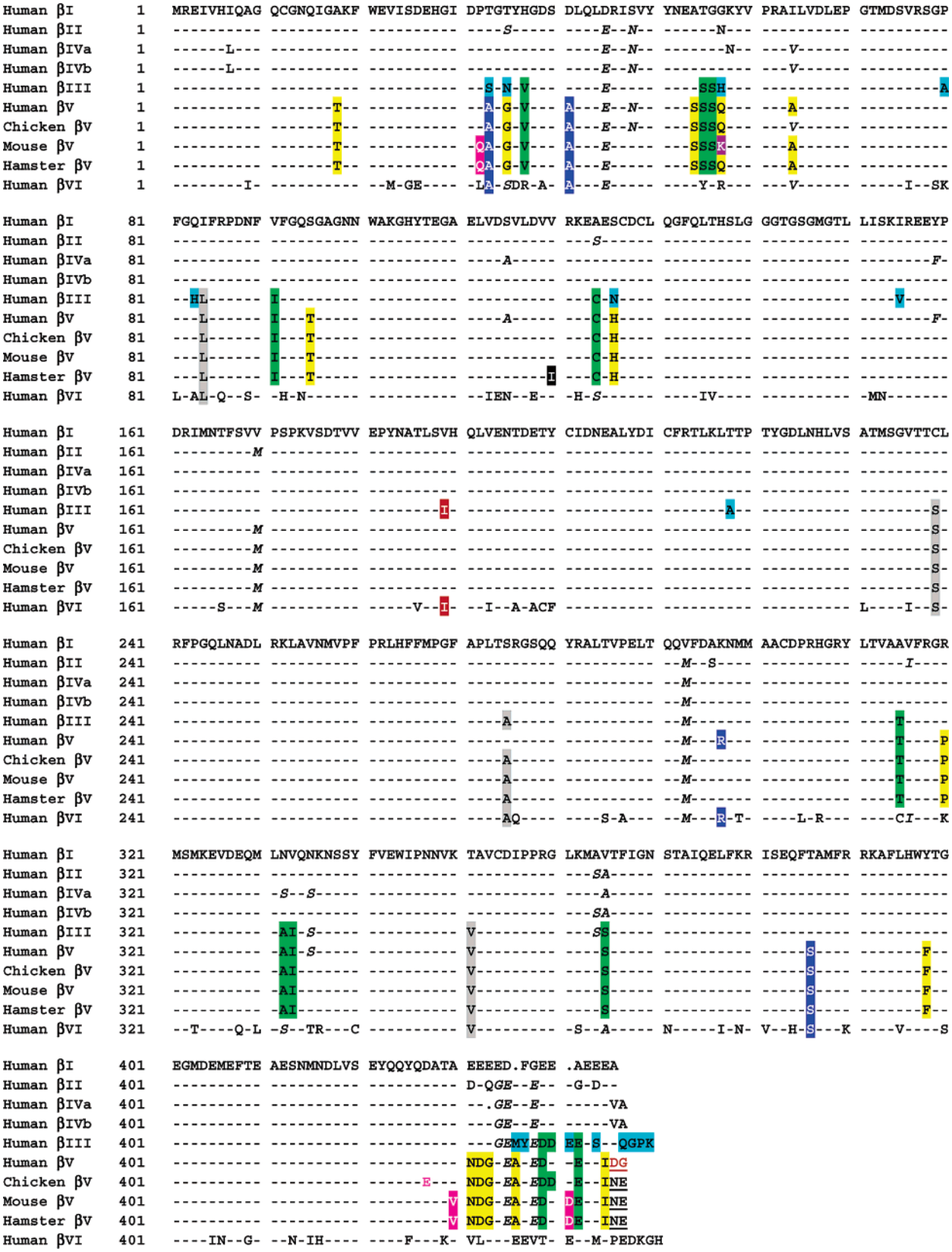

FIGURE 1: Alignment of human β-tubulin isotypes and chicken and rodent βV-tubulins. Human βV-tubulin sequence was obtained from cDNA libraries prepared from an endometrium and a breast carcinoma (NCBI accession numbers AAH02654 and Q9BUF5, respectively). The mouse βV-tubulin sequence was obtained from a cDNA library prepared from a mouse mammary tumor (*12*). Hamster βV-tubulin, partial sequence, was obtained from cDNA prepared from Chinese hamster ovary cells (*21*). Human βI-tubulin was used as the reference, and sequence divergences are highlighted in yellow (human βV-tubulins), turquoise (βIII-tubulin), blue (βV- and βVI-tubulin), gray (βIII-, βV-, and βVI-tubulin), red (βIII- and βVI-tubulin), black (hamster βV-tubulin), purple (mouse βV-tubulin), and pink (mouse and hamster βV-tubulin). Notice that one glutamate residue 427 specific to chicken βV-tubulin (*4*) is in pink and that the last two amino acids of human βV-tubulin are underlined in red and black for chicken and rodent βV-tubulins, respectively. Residues in italic are shared by isotypes belonging to the two divergent tubulin groups (see the text).

Table 1: Characteristics of Human Tubulin Isotypes and Rodent βV-Tubulin

tubulin isotype	accession number	isoelectric point	mass (Da)	CNBr C-terminal peptide	mass (Da) $[M-H]^-$
Kα1	AAC31959	4.94	50 151.6	AALEKDYEEVGVDSVEGEGEEEGEEY	2860.87
α3	Q13748	4.98	49 959.5	EEGEFSEAREDLAALEKDYEEVGVDSVEAEAEEGEEY	4152.21
α4	A25873	4.95	49 924.4	AALEKDYEEVG I D SYEDEDEGEE	2633.61
α6	Q9BQE3	4.96	49 895.3	AALEKDYEEVGADSADGEDEGEEY	2590.55
α8	Q9NY65	4.94	50 093.5	EEGEFSEAREDLAALEKDYEEVGTDSFEEENEGEEF	4158.17
βI	AAD33873	4.78	49 670.8	NDLVSEYQQYQDATAEEEEDFGEEAEEEA	3367.30
βII	AAH01352	4.78	49 953.1	NDLVSEYQQYQDATADEQGEFEEEEGEDEA	3467.28
βIII	AAH00748	4.83	50 432.7	YEDDEEESEAQGPK	1624.58
βIVa	NP_006078	4.78	49 585.8	NDLVSEYQQYQDATAEEGEFEEEAEEEVA	3351.35
βIVb	P05217	4.79	49 831.0	NDLVSEYQQYQDATAEEEGEFEEEAE E E V A	3480.46
βV	AAH02654/ Q9BUF5	4.77	49 857.1	NDLVSEYQQYQDATANDGEEAFEDEE E E I D G	3552.49
βVI	NP_110400	5.05	50 326.9	EPEDKGH	810.82
CHO/ mouse βV	AAZ14959/ Q922F4	4.76/ 4.80	50 104.3/ 50 090.4	NDLVSEYQQYQDATVNDGEEAFEDEDE E E I N E	3766.71

Microtubules containing only βIII-tubulin were less stable and were 2-fold more dynamic than microtubules made of βII- or βIV-tubulin (*6*) and were less sensitive to the suppressive effects of Taxol (*7*). Because the differences in assembly occurred in the absence of MAPs, these studies suggest that microtubule dynamics can be modulated by the intrinsic assembly properties of each β-tubulin isoform. Overexpression of βIII-tubulin moderately destabilizes microtubules in cells that are weakly resistant to Taxol (*8*) and reduces the ability of Taxol to suppress microtubule dynamics (*9*). Moreover, increased levels of βIII-tubulin are associated both *in vitro* and *in vivo* with intrinsic and acquired resistance to microtubule-interacting drugs. In the case of Taxol, these studies indicate that destabilization of microtubules by the presence of βIII-tubulin counteracts the microtubule stabilization and tubulin polymerization induced by Taxol (*10*). Recent data have indicated that overexpression of mouse βV-tubulin in CHO cells induces a significant loss of microtubule mass and dependence of cells on Taxol for normal growth (*11*).

Most of the tubulin profiling in mammalian cell lines and tissues has been achieved at the mRNA level by reverse transcriptase−polymerase chain reaction (RT-PCR) and at the protein level by antibody-based approaches (*10*). Human βV-tubulin has only been cloned recently (*12*, *13*), and its expression has not been described at the protein level. Despite the importance of microtubules for normal cell division and as a target for anticancer drugs, detailed information of human non-neuronal tubulin composition has been limited. Acidic peptides can be selectively detected by matrix-assisted laser desorption ionization−time-of-flight mass spectrometry (MALDI−TOF MS) in the negative mode (*14*). This property has been used to obtain mass spectra of tubulin C-terminal peptides from CNBr cleavage of tubulin from cancer cells. Prior to CNBr cleavage, tubulin was separated from other cytosolic proteins by sodium dodecyl sulfate−polyacrylamide gel electrophoresis (SDS−PAGE) and transferred onto nitrocellulose (*15*). In A549, a human nonsmall cell lung cancer cell line, and MDA-MB-231, a human breast cancer cell line, the major tubulin isotypes detected were Kα1- and βI-tubulin, along with βIVb-tubulin and a new α-tubulin, whose C-terminal sequence was determined by tandem mass spectrometry (MS/MS) and was found to be closely related to mouse α6-tubulin (*15*) (Table 1). In A549, the expression of βII-, βIII-, and βIVa-tubulin mRNAs was detected previously by RT-PCR (*16*). The apparent absence of their CNBr C-terminal peptides in negative-mode MALDI−TOF MS spectra indicated that the signals from these peptides were suppressed by other peptide ions. Purification of tubulin by Taxol-driven polymerization and the separation of α-tubulin from β-tubulin by long alkyl chain SDS−PAGE increased dramatically the βIVb-tubulin C-terminal peptide signal, but neither βII-, βIVa-, or βIII-tubulin C-terminal peptides were detected (*17*). Further separation of tubulin isoforms by high-resolution isoelectric focusing (IEF) and their identification by MALDI−TOF MS mass mapping or by the use of isotype specific antibodies was accomplished (*18*). Resolution of tubulin isoforms by reverse-phase HPLC coupled to ESI ion-trap MS determined their intact mass (*17*), confirmed the expression of βIII-tubulin, and detected the presence of α4-tubulin. Collectively, these three different mass-spectrometry-based analyses of tubulin from human cancer cell lines precisely identified which tubulin sequences were expressed in human cancer cell lines and revealed that α-tubulins were extensively tyrosinated and that a very small portion of α- and β-tubulin was monoglutamylated.

In the present study, the combination of tubulin isoform separation by high-resolution electrofocusing, in-gel cleavage of each isotype by CNBr, and analysis of the CNBr tubulin C-terminal peptides by MALDI−TOF MS in the negative mode allowed us to detect specifically and for the first time the protein expression of βV-tubulin in human cell lines.

MATERIALS AND METHODS

Chemicals and Cell Culture Media. Taxol was obtained from the Drug Development Branch of the National Cancer Institute (Bethesda, MD) and dissolved in sterile dimethyl sulfoxide and stored at −20 °C. All other chemicals were obtained from Sigma (St. Louis, MO), except where noted. RPMI 1640, αMEM, DMEM, and 199 media were obtained from Invitrogen (Carlsbad, CA), and MCDB105 medium was from Sigma (St. Louis, MO).

Cell Culture and Cytotoxicity Assay. The human A549 lung cell line and Hey ovarian cell line were maintained in RPMI 1640 with 10% fetal bovine serum (FBS). The human IOSE cell line (generous gift from Dr. N. Auersperg, University of British Columbia, Vancouver, British Columbia, Canada) was maintained in a 1:1 mixture of medium 199/MCDB105 containing 5% FBS and 50 μg/mL gentami-

cin. The CHO cell line was maintained in αMEM, 1% penicillin/streptomycin, and 10% FBS. The mouse ovarian ID8 cell line (generous gift from Dr. K. F. Roby, University of Kansas Medical Center, Kansas City, KS) was maintained in DMEM, 4% FBS, 1% penicillin/streptomycin, 5 μg/mL insulin, 5 μg/mL transferrin, and 5 ng/mL selenite (ITS mix from Sigma, St. Louis, MO). Cytotoxicity was determined using the MTS assay from Promega (Madison, WI) after a 72 h treatment with Taxol or vinblastine.

Isolation of Tubulin from Cell Lines. Tubulin was isolated from all cell lines by inducing its polymerization with Taxol and pelleting the resulting Taxol-stabilized microtubules as described previously (*19*).

Isoelectrofocusing. Taxol-stabilized microtubules were resuspended in IEF sample buffer, and solubilized tubulins were loaded on 18 or 24 cm immobilized pH gradient (IPG) strips at pH 4.5−5.5 (GE Health, Piscataway, NJ) that were run on an IPGphor IEF system (GE Health, Piscataway, NJ) as described previously (*18*). IPG strips were stained with Coomassie blue or an imidazole-zinc staining procedure that is compatible with direct chemical cleavage or enzymatic digestion as described previously (*18*). Image analysis of stained gels was performed using ImageJ software.

In-Gel CNBr Cleavage and Analysis of Tubulin C-Terminal Peptides. IEF gel bands containing tubulin were cut out and transferred to an Eppendorf tube and washed twice with 150 μL of an aqueous solution of 50% acetonitrile at 30 °C for 20 min. The gel pieces were removed, dried in a speed-vac, and rehydrated with 100 μL of a 100 mg/mL CNBr solution in 70% formic acid. The CNBr cleavage was performed in the dark at room temperature for 24 h. The gel piece was removed, and the solution containing the peptides generated by CNBr cleavage was completely evaporated in a speed-vac. Peptides were dissolved in 100 μL of a 50% acetonitrile and 0.3% TFA solution, and the solution was evaporated. This was repeated once. The final residue was dissolved in 10 μL of a 50% acetonitrile and 0.3% TFA solution and diluted 1:5 and 1:10 in the same solution. An aliquot of 1 μL of each dilution was mixed with 1 μL of sinapinic acid for MALDI−TOF MS analysis in the negative mode as described previously (*15*).

In-Gel Trypsin Digestion and Analysis of Tryptic Peptides. IEF gels were stained with Coomassie blue as described previously (*18*) and destained until the background was minimal. Bands containing tubulin were cut out and washed twice with water and destained in 300 μL of destaining solution (200 mM ammonium bicarbonate/50% acetonitrile at pH 8.9). After the complete loss of color, 300 μL of acetonitrile was added, and after vortexing and sonicating for 10 s, the supernatant was removed and each gel piece was dried down in a Speed-Vac. For reduction, the gel piece was swelled with 300 μL of 10 mM dithiothreitol (DTT) in 0.1 M ammonium bicarbonate, incubated for 45 min at 56 °C, and cooled at room temperature and an excess of liquid was removed. For alkylation, the gel piece was covered with 300 μL of 55 mM iodoacetamide in 0.1 M ammonium bicarbonate, incubated for 30 min at room temperature in the dark. Iodoacetamide solution was removed, and the gel piece was washed twice with 300 μL of 1:1 acetonitrile/200 mM ammonium bicarbonate solution. Acetonitrile was added on the gel piece, and after vortexing and sonicating for 10 s, the supernatant was removed and each gel piece was dried in a Speed-Vac. Then, trypsin digestion and preparation of the tryptic peptide mixture were used for MALDI−TOF or MALDI−TOF/TOF MS analysis as described previously (*18*), except that PepClean C-18 Spin Columns (Pierce, Rockford, IL) were used instead of C18 Ziptip (Millipore, Billerica, MA) following the instructions of the manufacturer.

Stable Isotope Labeling with Amino Acids in Culture (SILAC). The SILAC method (*20*) was used to label the cellular protein content. RPMI 1640 medium lacking leucine (USBiological, Swampscott, MA) was supplemented with dialyzed serum (Gemini Bio-Products, Woodlands, CA) and with either regular L-leucine (d0-Leu) or L-leucine labeled with three deuteriums (d3-Leu) (Sigma−Aldrich, St. Louis, MO). Hey cells were cultured in d3-Leu-containing medium, and A549 cells were cultured in d0-Leu-containing medium. After incorporation for five doubling times, equal amounts of soluble proteins were isolated from both cultures and mixed in equal amounts. Tubulin was isolated, and tubulin isotypes were separated on 24 cm IEF gels and digested by trypsin as described above. MALDI−TOF MS analysis was performed using a ABI 4700 TOF/TOF mass spectrometer (Applied Biosystem, Foster City, CA). Dependent upon the number of leucine residues in a tryptic peptide, the peptide is represented by a doublet of peaks separated by a multiple of 3 Da in the mass spectra. The signal intensity of each peak in the doublet is used to calculate the relative abundance of a tubulin isotype in Hey versus A549 cells. We observed a small but detectable fraction of partially labeled peptides in Hey cells (see Figure 7B). Therefore, a correction factor for isotopic overlap was applied to each peptide to determine the quantitative ratios of d3-Leu to d0-Leu peptides. Because the partially labeled d3-Leu peptide peak can only be contributed from the Hey cell line grown in d3-Leu supplemented media, each of the partially labeled d3-Leu peptide peaks was deconvoluted and added to the corresponding fully labeled d3-Leu peptide peak. Isopro software was used to calculate the isotopic distribution of each peptide. After normalization to the height of the monoisotopic peak of the d0-Leu peptide, the value was subtracted from the full isotope pattern to obtain the real monoisotopic height of the partially d3 Leu substituted peak. This height was then added to the fully labeled d3-Leu peptide peak to obtain the corrected monoisotopic peak height. The correction factor was calculated using the sequence of peptide $_{241}$FPGQL-NADLR$_{251}$ (*m*/*z* 1130.65) and was consistently 1.1 in several spectra. This correction factor was applied for the calculation of all of the ratios of d3-Leu/d0-Leu peptide.

Liquid Chromatography Coupled to Electrospray Ionization Mass Spectrometry (LC/ESI MS). Tubulins present in Taxol-stabilized microtubule pellets were separated by HPLC, and their mass was determined using an ion-trap mass spectrometer as described previously (*17*).

Western Blot Analysis. Cells, ∼90% confluent, were collected from one 100 mm Petri dish, washed with phosphate-buffered saline (PBS), and lysed in 50 μL of 1% SDS in PBS for 15 min on ice. Total lysates were flash frozen in liquid nitrogen and kept at −20 °C. Lysates were thawed; the protease inhibitor cocktail (Roche, Basel, Switzerland) was added; and the lysates were centrifuged at 14 000 rpm for 3 min. Supernatants were collected, and protein levels were measured by the Lowry assay. A total of 20 μg of protein/lane were run on a 10% SDS−PAGE gel and

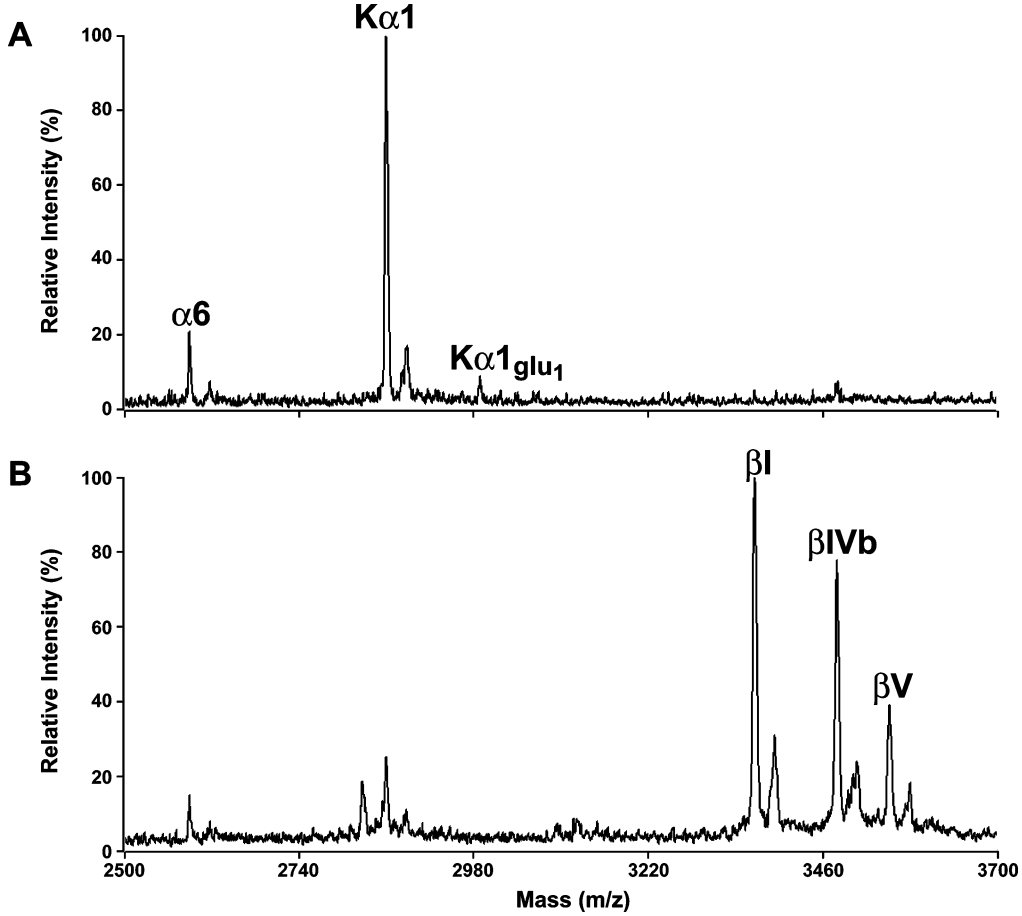

FIGURE 2: Detection of CNBr C-terminal peptide from human βV-tubulin by MALDI−TOF MS. α- and β-tubulins from Hey cells were separated, and CNBr C-terminal peptides from the α-tubulin fraction (A) and from the β-tubulin fraction (B) were detected by MALDI−TOF MS analysis in the negative mode. The small mass peaks systematically present after each tubulin C-terminal peptide with a +28-Da Δmass are most likely due to their formylation by a trace amount of formaldehyde present in the formic acid−CNBr solution. After internal calibration with the βI-tubulin C-terminal peptide (*m*/*z* 3367.30), the *m*/*z* value for βIVb-tubulin C-terminal peptide was 3480.50 and the *m*/*z* value for human βV-tubulin was 3552.45 (Δ*m*/*z* with theoretical values = ±40 ppm, see Table 1). After internal calibration with the Kα1-tubulin C-terminal peptide (*m*/*z* 2860.87), the *m*/*z* value for α6-tubulin C-terminal peptide was 2590.49 (Δ*m*/*z* with theoretical values = −60 ppm, see Table 1).

transferred to a nitrocellulose membrane, probed with a pan-β-tubulin antibody (DM1-B, Sigma, St. Louis, MO), followed by a goat anti-mouse secondary antibody conjugated to horseradish peroxidase (HRP), and analyzed by enhanced chemoluminescence (ECL) (Amersham Biosciences, Piscataway, NJ). The membrane was stripped, reprobed with an anti-βIII-tubulin antibody (Sigma, St. Louis, MO), and processed as described. Autoradiogram films were scanned, and the signal for each band was integrated using the image analysis software ImageJ (NIH).

RESULTS AND DISCUSSION

Sequence Specificities of Human βV-Tubulin. The alignment of human β-tubulin sequences, including the recently cloned βV-tubulin sequence (*12*, *13*) with chicken (*4*), mouse (*12*), and hamster βV-tubulin sequences (*21*) clearly showed that βV-tubulin is distinct from the other isotypes and is closely related to βIII-tubulin and to a lesser extent to βVI-tubulin (βV- versus βIII-tubulin, 45.2% of identical sequence divergence from βI-tubulin; βV- versus βVI-tubulin, 28.6%; βV- versus βIVa-tubulin, 19.0%; βV- versus βII-tubulin, 14.3%; and βV- versus βIVb-tubulin, 9.5%) (Figure 1). In chicken, rodent, and human βV-tubulin, 85.7% of sequence divergence from βI-tubulin is conserved. The two last amino acid residues of human βV-tubulin differ from the corresponding bird and rodent residues. This is indicative of the evolutionary pressure that may have provided specific functions to human βV-tubulin because human and mouse βI-, βII-, βIII-, βIVa-, or βIVb-tubulins have identical extreme C-termini. Mouse and human βI-, βII-, βIVa-, or βIVb-tubulin are 100% identical, whereas mouse and human βIII-, βV-, or βVI-tubulin display 99.8, 97.7, and 91.1% identity, respectively (data not shown). Collectively, these characteristics of the recently cloned human βV-tubulin sequence (*12*, *13*) required confirmation at the protein level.

High Level of Expression of Human βV-Tubulin in an Ovarian Cell Line. Human βV-tubulin sequence has been entered only recently in the NCBI protein database after high throughput sequencing of human cDNA libraries from an endometrial adenocarcinoma (*12*) and from breast (*13*). We isolated tubulin from Hey, an epithelial ovarian cancer cell line, and α-tubulin was separated from β-tubulin by electrophoresis prior to their cleavage by CNBr. The C-terminal peptides were analyzed by MALDI−TOF MS in the negative mode (Figure 2). As observed previously (*17*), this approach improved significantly the signal-to-noise ratio of C-terminal peptides from βIVb-tubulin and possibly from other β-tubulin isotypes. As in other cancer cell lines, the α-tubulin fraction

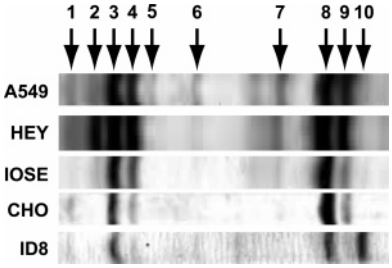

FIGURE 3: Separation of tubulin isotypes from epithelial cells lines by high-resolution IEF. Tubulin was isolated from A549, Hey, IOSE, or CHO cell lines. Tubulin isotypes were resolved on IEF gels that were subsequently stained with Coomassie blue. Each individual band is indicated by a numbered arrow: 1, monoglutamylated βI-tubulin (pI 4.76); 2, monoglutamylated βIVb-tubulin and human βV-tubulin (pI 4.77); 3, βI-tubulin (pI 4.78); 4, βIVb-tubulin (pI 4.79); 5, monoglutamylated βIII-tubulin (pI 4.81); 6, βIII-tubulin (pI 4.83); 7, monoglutamylated Kα1-tubulin (pI 4.92); 8, Kα1-tubulin (pI 4.94); 9, α6-tubulin (pI 4.96); and 10, unknown γ-actin isoform (predicted pI 4.98).

contained α6 and Kα1 isotypes (Figure 2A), but in the β-tubulin fraction, in addition to the βI and βIVb isotype C termini, an additional smaller mass peak at 3552.5 Da was readily detected and tentatively assigned to the predicted βV-tubulin C-terminal peptide (Table 1 and Figure 2B). Despite the fact that peptides may have a differential ionization potential, we measured the area under the peaks of βI-, βIVb-, and βV-tubulin and the results indicated that βV-tubulin could represent 18% of β-tubulin in Hey cells.

The calculated isoelectric point for βV-tubulin is 4.77, which locates human βV-tubulin to the left of βI-tubulin [isoelectric point (pI) 4.78] at a distance equivalent to that between βIVb-tubulin (pI 4.79) and βI-tubulin (pI 4.78). A band with an intensity similar to the βIVb-tubulin band was located at that exact position for tubulin isolated from Hey cells (arrow 2 in Figure 3). Only a faint band was observed at that position for tubulin from A549 cells and from human immortalized normal ovarian surface epithelial cells (IOSE). Tubulin from a mouse ovarian cancer cell line, ID8 (*22*), was also analyzed by IEF (Figure 3), and the band pattern was undistinguishable from that of CHO cells, except that an additional band (band 10 in Figure 3) was strongly stained and was potentially an α-tubulin. Analysis of this band by MS/MS revealed that it did not contain α-tubulin but γ-actin (data not shown), which should focus at a more basic pI (5.3). The reason for that shift to a significantly more acidic pI and the function of this unknown isoform of γ-actin will be described elsewhere. We previously reported the presence of actin in Taxol−microtubule pellets prepared from cell lines (*18*). To correlate our data on CNBr C-terminal peptides and the presence of a strong Coomassie stained band at the expected focusing site for human βV-tubulin, we performed CNBr cleavage of each tubulin-containing IEF gel band after imidazole-zinc staining of IEF strips and analyzed the produced peptides by MALDI−TOF MS in the negative mode (Figure 4). In Hey cells, we clearly detected a major mass peak at 3552.5 Da corresponding to human βV-tubulin C-terminal peptide after CNBr in-gel cleavage of the IEF gel band presumed to contain βV-tubulin (arrow 2 in Figure 3 and Figure 4). The same mass peak was present but as a minor species, when the same analysis was performed on tubulin from IOSE and A549 cells (Figure 5), and it was below detectable levels in MDA-MB-231 breast cancer cells (data not shown). A comparison of mass peak intensities of βV- and βI-tubulin C-terminal peptides from Hey (band 2 in Figure 4), A549, and IOSE cell lines (Figure 5) indicated that βV-tubulin could be approximately 2−3-fold more abundant in Hey than in A549 or IOSE cell lines. Human βV-tubulin has the same pI as monoglutamylated βIVb-tubulin. A mass peak at 3609.9 Da was present in the mass spectrum of the peptides generated by CNBr cleavage of the band containing βV-tubulin that matched the calculated mass of βIVb-tubulin C-terminal peptide with one additional glutamate residue (Figure 4). Despite careful cutting of each band, cross-contamination of bands obviously occurred (Hey bands 2 and 3 in Figure 4). βI-Tubulin, being the major β-tubulin, contaminated other neighboring bands most likely because of unfocused βI-tubulin present at the edges of the IEF strip. Nevertheless, the presence of the C-terminal peptide from βI-tubulin in all of the spectra allowed internal mass calibration. We readily detected the C-terminal peptides of monoglutamylated Kα1-tubulin (arrow 7 in Figure 3), Kα1-tubulin (arrow 8 in Figure 3) and α6-tubulin (arrow 9 in Figure 3) (data not shown). The band 1 in A549, Hey, CHO, and ID8 cell lines (Figure 4) contained monoglutamylated βI-tubulin (data not shown) but was not detectable in the IOSE cell line. Monoglutamylated βV-tubulin should focus at pI 4.75, but we could not detect this band by Coomassie blue staining. Nevertheless, we observed previously monoglutamylated β- and α-tubulin in other cell lines (*17*, *18*), and we speculate that a small portion of monoglutamylated βV-tubulin is also present in cancer cell lines. Additionally, there is, thus far, no indication of differential glutamylation of α- versus β-tubulin or of the different isotypes (*23*). As observed previously, detyrosinated α-tubulin was under detectable levels in any of the cell lines (*17*, *18*).

The rodent βV-tubulin C-terminal peptide is distinct from its human counterpart (Table 1 and Figure 1). Hamster βV-tubulin focuses with monoglutamylated βI-tubulin (arrow 1 in Figure 3) and mouse βV-tubulin focuses between βIVb- and monoglutamylated βIII-tubulin (*18*) (arrows 4 and 5 in Figure 3). Cleavage of these bands from CHO and ID8 cells by CNBr confirmed the presence of the rodent βV-tubulin C-terminal peptide (Figure 4). Expression of Chinese hamster βV-tubulin has been observed in CHO cells by second dimension (2D) gel electrophoresis and Western blotting, and the amount of βV-tubulin in these cells was estimated to represent about 7% of the total β-tubulin in CHO cells (*24*).

The band containing βIII-tubulin from A549 (arrow 6 in Figure 3) yielded only a very weak signal, just above noise; however, it corresponded to the mass of CNBr βIII-tubulin C-terminal peptide at 1625 Da (data not shown). We could not detect the monoglutamylated C-terminal peptide of βIII-tubulin in band 5. However, previous IEF Western blots with an antibody specific for this isotype and LC−MS of A549 tubulin (*17*, *18*), showed that both βIII-tubulin and monoglutamylated βIII-tubulin were expressed. βIII-tubulin can be phosphorylated (*2*), and we cannot exclude the expression of this isoform of βIII-tubulin in Hey cells, in which case it should focus at a more acidic pI position than band 5. Alternatively, we evaluated the levels of expression of βIII-tubulin in ovarian cells compared to A549 cells by Western blot analysis (Figure 6) utilizing a highly specific anti-βIII-tubulin antibody (*18*). Consistent with the relative intensity

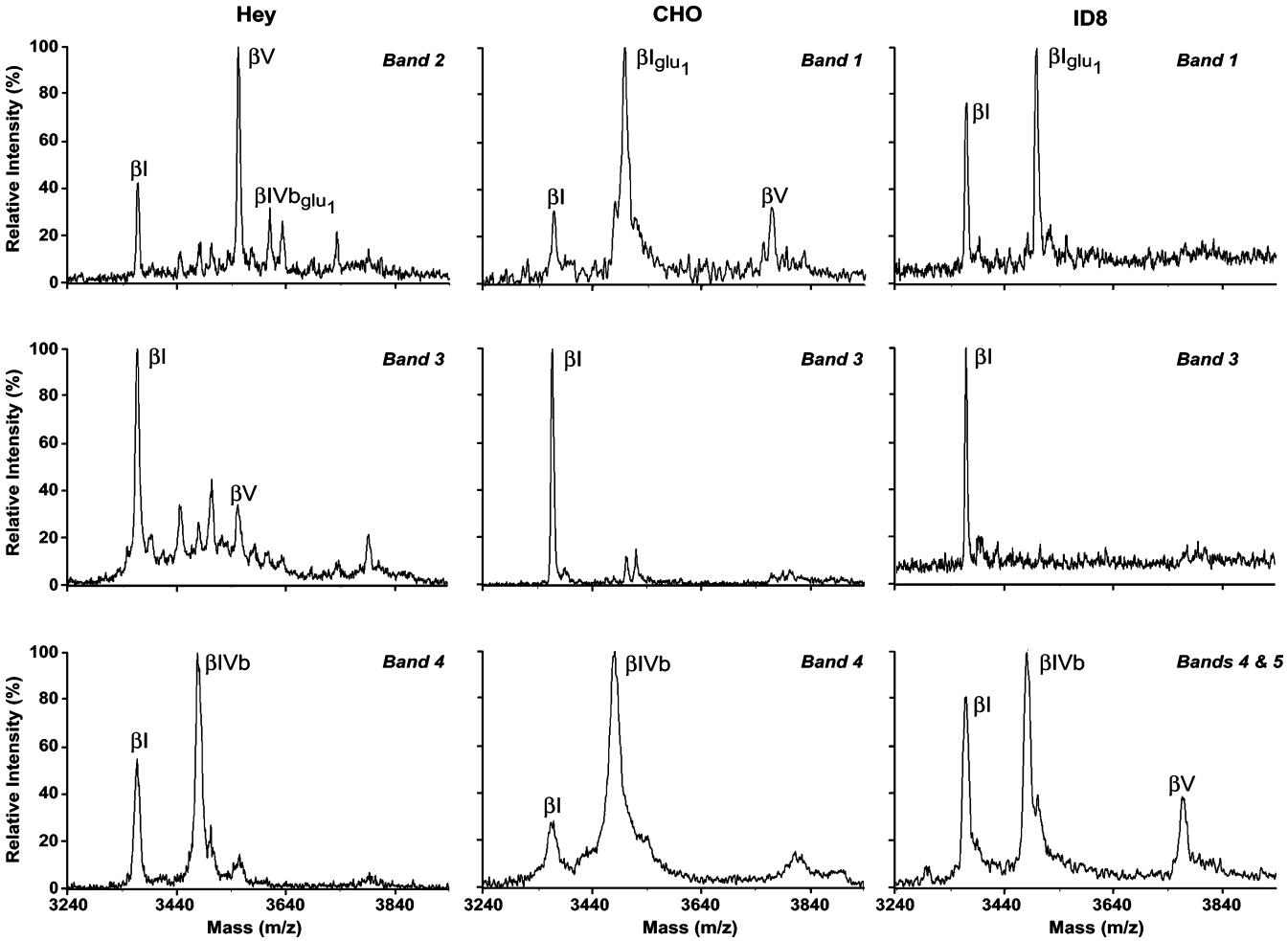

FIGURE 4: Detection of C-terminal peptides by MALDI−TOF MS after CNBr in-gel cleavage of tubulin isotypes resolved by IEF. Tubulin isoforms from Hey cells (left column), from CHO cells (middle column), or from ID8 cells (right column) were resolved by IEF. IEF gel bands containing tubulin were cut and incubated in the presence of CNBr, and the released tubulin C-terminal peptides were analyzed by MALDI−TOF MS in the negative mode. The band number used in Figure 3 is indicated in the top right corner of each mass spectrum. Because no band was visible where mouse βV-tubulin was expected to focus (between bands 4 and 5), the piece of gel including these two bands was analyzed. After internal calibration with the βI-tubulin C-terminal peptide (*m*/*z* 3367.30), the average *m*/*z* value for monoglutamylated βI-tubulin C-terminal peptide (βI_{glu1}) was 3496.6; for βIVb-tubulin, 3480.50; for monoglutamylated βIVb-tubulin (βIVb_{glu1}), 3609.9; for human βV-tubulin, 3552.5; and for rodent βV-tubulin, 3766.2 (see Table 1 for theoretical values. A mass of 129 Da has to be added for monoglutamylated isoforms).

of Coomassie stained bands on IEF gels presented in Figure 3 (arrow 6), Hey expressed almost undetectable levels of βIII-tubulin, whereas it was readily detected in A549 cells. IOSE cells expressed detectable but lower levels of βIII-tubulin. Consistent with the analysis of βIII-tubulin in CHO cells by others (*24*), we did not detect this isotype in these cells or in the mouse ID8 cells (Figure 6).

Increased resolution of tubulin isotypes from Hey and A549 cells on IEF gels was required to perform a more accurate relative quantitation of βV-tubulin expression in these cells. Therefore, 24 cm IEF gel strips at pH 4.5−5.5 were used, and after staining with Coomassie, the separation between tubulin isotypes was significantly improved (Figure 7A). It was again apparent that βV-tubulin was expressed at higher levels in Hey than in A549, whereas βIII-tubulin was expressed at lower levels. The band containing βV-tubulin was reduced, alkykated, and digested by trypsin for identification by MALDI−TOF MS peptide mapping (Table 2). Specific βV-tubulin tryptic peptides were detected, whereas βI- or βIVb-tubulin tryptic peptides were not, indicating that βV-tubulin is the major tubulin species in that band. To address the possibility that the higher expression of βV-tubulin in Hey cells was in fact reflecting a general increase in tubulin expression in Hey cells, SILAC experiments (*20*) were performed (Figure 7B). Proteins in Hey cells were labeled in culture with leucine containing three deuteriums (d3-Leu), whereas proteins in A549 were synthesized in the presence of unlabeled leucine (d0-Leu). After equal amounts of soluble proteins obtained from each cell line were mixed, Taxol-driven isolation of tubulin and IEF separation of tubulin isotypes were carried out (Figure 7A). Tryptic digests of each isotype were analyzed by MALDI−TOF MS (Figure 7B). Height ratios of d3-Leu-labeled peptides from Hey cells versus d0-Leu peptides from A549 cells were calculated for βV-, βI-, and βIVb-tubulin using isotype specific and common peptides (Figure 7C). This analysis allowed the detection of a slighty higher expression of βI- and βIVb-tubulin (1.4- and 1.5-fold, respectively) in Hey cells (Figure 7C). These β-tubulin isotypes represent at least 80% of β-tubulin in the two cell lines; therefore, this result suggests that Hey cells expressed more tubulin than A549 cells. However, the analysis of tubulin isotype-specific peptides

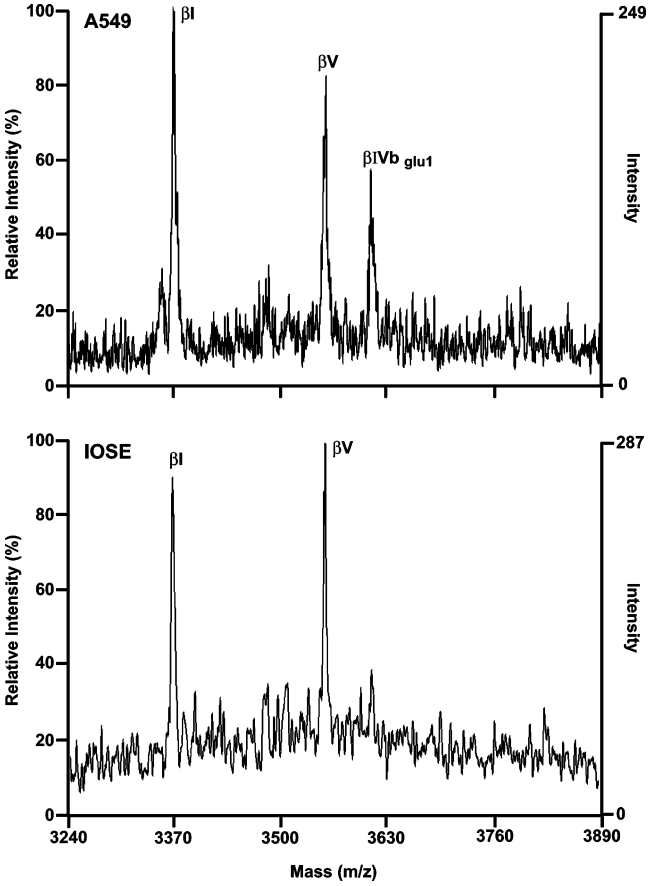

FIGURE 5: Detection of βV-tubulin C-terminal peptides from A549 and IOSE cell lines by MALDI−TOF MS. Tubulin isoforms from A549 cells (top panel) or from IOSE cells (bottom panel) were resolved by IEF. IEF gel band 2 containing βV-tubulin was cut and incubated in the presence of CNBr, and the released tubulin C-terminal peptides were analyzed by MALDI−TOF MS in the negative mode. After internal calibration with the βI-tubulin C-terminal peptide (*m*/*z* 3367.30), the average *m*/*z* value for βV-tubulin C-terminal peptide (βV) was 3552.43 and the average *m*/*z* value for monoglutamylated βIVb-tubulin (βIVb_{glu1}) was 3609.15. Maximal intensities are indicated on the right vertical axis; for comparison, the maximal intensity of βV-tubulin C-terminal for Hey cells (band 2 of Figure 4) was 862.

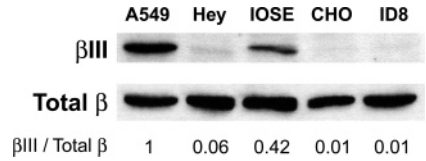

FIGURE 6: Western blot analysis of βIII-tubulin expression in the A549 lung cancer cell line and in ovarian cancer cell lines. A total of 30 μg of total proteins was separated on a 10% acrylamide gel and transferred onto a nitrocellulose membrane. The membrane was first probed for βIII-tubulin, stripped, and reprobed with DM1-B, a pan-β-tubulin antibody. The calculated βIII-tubulin/total β-tubulin signal ratio are presented in arbitrary units, and values have been normalized using a ratio of 1 for A549 cells.

revealed a 3.8-fold higher expression of βV-tubulin in Hey cells (top panel of Figure 7C). A lower ratio of 2.6-fold and larger standard deviation was observed when both βV-tubulin isotype-specific and common peptides were used for the calculation (lower panel of Figure 7C). This is most likely resulting from the presence of a small amount of monoglutamylated βIVb-tubulin in the IEF gel band containing βV-tubulin, and despite a better resolution of tubulin isotypes on 24 cm IEF gels, cross-contamination by βI-tubulin could still occur. In any case, this difference in βV-tubulin expression was statistically significant using both methods of calculation. The same analysis on the βIII-tubulin band was not achievable, because the βIII-tubulin band in IEF gels from SILAC experiments was not stained by Coomassie blue. This is most likely due to the dilution of βIII-tubulin from A549 by Hey tubulin, which contains almost no βIII-tubulin.

Collectively, our analysis of βIII- and βV-tubulin expression at the protein level suggests that a highly regulated balance between βIII- and βV-tubulin expression could occur in cells. This is reminiscent of the distribution of βIII- and βV-tubulin mRNA observed in chicken cell lines and tissues (*4*). Therefore, such a complementary pattern of expression of βIII- and βV-tubulin may be conserved in vertebrates from birds to humans. We speculate that the combined expression of βIII- and βV-tubulin, for normal cell function, may not exceed about 20% of the total β-tubulin, which would explain why these two β-tubulin isotypes represent minor species in cells in culture and tissues.

To confirm that the sequence of human βV-tubulin entered in the NCBI protein database is correct beyond the C-terminal sequence, we analyzed tubulin from Hey cells by LC−MS (*17*) to measure the mass of the intact βV-tubulin protein (Figure 8). Mass peaks corresponding to βIVb-tubulin and α6-tubulin were clearly resolved in our previously published deconvoluted spectrum of tubulin from A549 (*17*). In contrast, a mass peak was observed filling in the valley between βIVb- and α6-tubulin mass peaks in an equivalent deconvoluted spectrum of Hey tubulins (Figure 8A). This was expected because the calculated mass of human βV-tubulin (49 857 Da) is intermediate between the masses of βIVb- and α6-tubulin (Table 1). When the mass peaks were deconvoluted in segments of retention times, the presence of an additional deconvoluted mass peak at 49 845 Da was clearly apparent (Figure 8B). This mass is only 12 Da lower than the calculated mass for βV-tubulin, which is in the range of the systematic −9 to −12 Da difference that we observed previously with the other tubulin isoforms (*17*).

Collectively, these results demonstrate that the human βV-tubulin sequence present in the NCBI protein database is effectively expressed at the protein level in epithelial cells. Protein expression of human βV-tubulin will need to be examined in a broader set of cell lines and in normal and malignant tissues to assess its level of expression in comparison to βIII-tubulin. This would be achievable with antibodies against human βV-tubulin. The specificity of such immunological tools could be easily tested using the tubulin proteomics approaches developed in our laboratory (*18*).

Potential Role of Human βV-Tubulin in Microtubule Dynamics and in Response to Microtubule-Interacting Agents. Tubulin isotype composition has been shown to alter microtubules dynamics both *in vitro* and in cells (*10*). In particular, overexpression of βIII-tubulin (*8*) and of mouse βV-tubulin (*11*) in CHO cells destabilizes microtubules. Despite the possible involvement of the C-terminus of these tubulin isotypes in the alterations of microtubule dynamics, it is most likely the sequence divergence at sites that are involved in tubulin dimer−dimer interactions that influences the overall stability of microtubules. The model of a tubulin hetetodimer (*25*) and its docking in a 3D reconstruction of high-resolution electron microscopy images of a microtubule

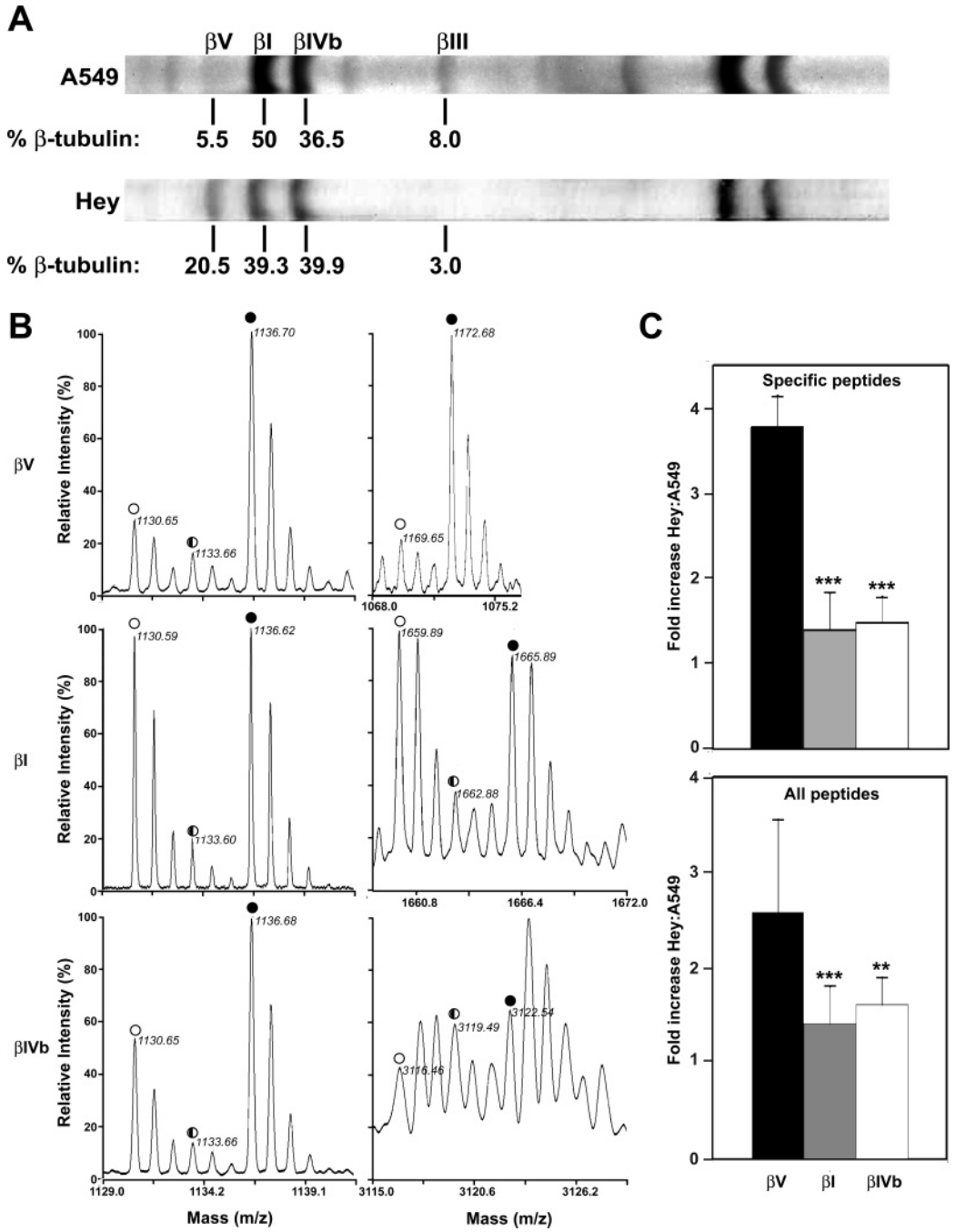

FIGURE 7: Relative quantitation of βV-tubulin expression in Hey and A549 cells. (A) Higher resolution of tubulin isotypes from Hey and A549 cells lines was achieved on 24 cm IEF gels at pH 4.5−5.5. IEF gels were stained with Coomassie blue, and relative quantitation of βV-, βI-, βIVb-, and βIII-tubulin was performed by image analysis of each band. The percentage of each β-tubulin isotype in total β-tubulin is indicated at the bottom of each strip. (B) Following SILAC, equivalent amounts of total soluble d3-Leu-labeled proteins from Hey and of unlabeled (d0-Leu) total soluble proteins from A549 were mixed and used to prepare Taxol microtubules. Tubulin isotypes were separated on 24 cm IEF gels and digested by trypsin, and tryptic peptides were analyzed by MALDI−TOF MS. Peptides containing leucine were used to measure the ratio of βV-, βI-, and βIVb-tubulin in Hey versus A549 cells. Such a peptide, $_{242}$FPGQLNADLR$_{251}$ (*m*/*z* 1130.59) common to these three isotypes, is presented (left column), and a peptide specific for each isotype is presented (right column; βV-tubulin, $_{310}$YLTVATVFR$_{318}$, *m*/*z* 1069.60; βI-tubulin, $_{283}$ALTVPELTQQVFDAK$_{297}$, *m*/*z* 1659.89; βIVb-tubulin, $_{20}$FWEVISDEHGIDPTGTYH-GDSDLQLER$_{46}$, *m*/*z* 3116.42). Unlabeled peptides (○), half-labeled peptides (◐), and fully labeled peptides (●). (C) Calculated Hey:A549 tubulin isotype ratio using tubulin isotype-specific peptides (top panel) or these peptides plus all of the other detectable leucine-containing peptides. A correcting factor was used to add the height of half-labeled peptide mass peaks to the height of fully labeled peptides (see the Materials and Methods for details). Average values ± SD from two independent experiments are presented. Specific peptides, (***) $p = 0.0002$. All peptides, (**) $p = 0.005$; (***) $p < 0.0001$ (two-tailed Student's *t* test), as compared to βV-tubulin Hey/A549 ratio.

(*26*, *27*) identified more precisely the tubulin structural domains involved in lateral contacts between tubulin dimers in adjacent protofilaments. The M and H10−S9 loops from the α- and β-tubulin monomers form a domain that is predicted to interact with the long flexible H1−S2 loop of the adjacent α- and β-tubulin monomers (Figure 9). Moreover, the expression of a single mutation at position 60 situated at the end of the H1−S2 loop on βI-tubulin, from a valine to an alanine residue, induced Taxol dependence (*28*). A cell line highly dependent upon epothilone B that bears a

Table 2: Analysis of Tryptic Digest from Human βV-Tubulin-Containing Band by MALDI−TOF Mass Spectrometry

βV-tubulin-isotype-specific peptides[a]	measured mass of peptide	calculated mass of peptide	Δmass (Da)	protein determination[b]
$_{351}$VAVCDIPPR$_{359}$	1026.57	1026.54	0.03	
$_{310}$YLTVATVFR$_{318}$	1069.65	1069.60	0.05	
$_{381}$ISEQFSAMFR$_{390}$	1215.62	1215.58	0.04	
$_{381}$ISEQFSAMFR$_{390}$ (MSO)	1231.61	1231.58	0.03	
$_{47}$INVYYNESSSQK$_{58}$	1431.72	1431.67	0.05	βV-tubulin
$_{63}$AALVDLEPGTMDSVR$_{77}$	1573.83	1573.79	0.04	sequence coverage: 40%
$_{63}$AALVDLEPGTMDSVR$_{77}$ (MSO)	1589.82	1589.78	0.04	
$_{283}$ALTVPELTQQMFDAR$_{297}$	1719.90	1719.87	0.03	
$_{283}$ALTVPELTQQMFDAR$_{297}$ (MSO)	1735.89	1735.87	0.02	
$_{3}$EIVHIQAGQCGNQIGTK$_{19}$	1852.95	1852.93	0.03	
$_{1}$MREIVHIQAGQCGNQIGTK$_{19}$	2140.10	2140.07	0.03	
$_{1}$MREIVHIQAGQCGNQIGTK$_{19}$ (MSO)	2156.08	2156.07	0.01	

[a] Identified peptides and combination of peptides specific for βV-tubulin isotype. MSO, oxidized methionine; CAM, carbamidomethylated. [b] Sequence coverage was calculated on the basis of all of the matched tryptic peptides, i.e., tubulin-isotype-specific and nonspecific peptides detected. Protein identification was performed by using all detected peptides and MS-Fit software (Protein Prospector, UCSF, San Francisco, CA) and NCBI protein database.

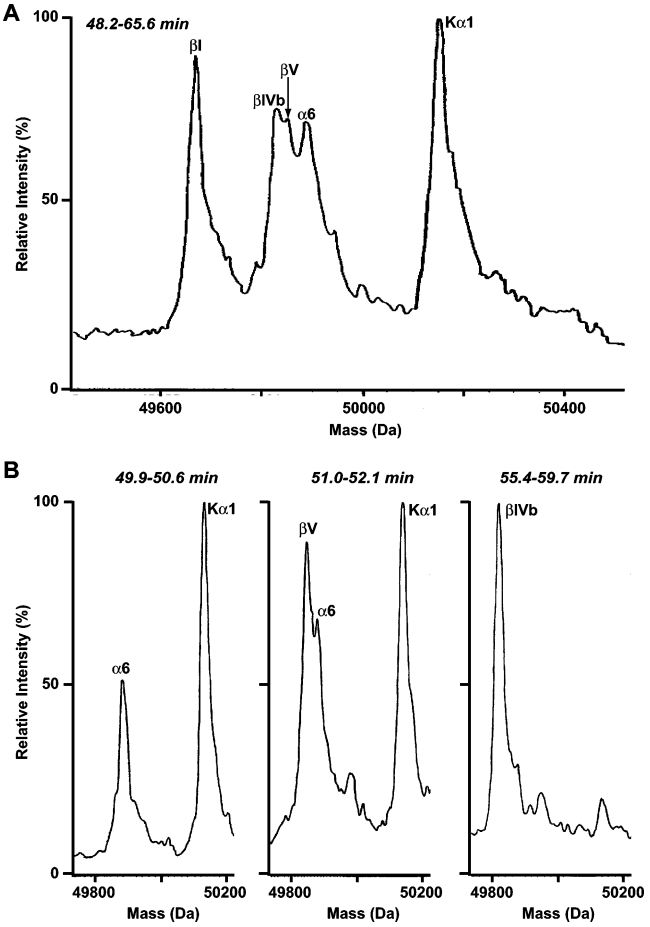

FIGURE 8: Analysis of intact tubulins from Hey cells by LC/ESI MS. Tubulin isoforms isolated from Hey cells were separated by reverse-phase chromatography, and their elution was monitored with an ESI ion-trap mass spectrometer. (A) Deconvoluted mass spectrum corresponding to retention times (48.2−65.6 min) at which tubulin was eluting. (B) Deconvoluted mass spectra of tubulin isotypes eluting at the indicated times of retention. The average mass was 49 659.5 Da for βI-tubulin, 49 818.5 Da for βIVb-tubulin, 49 845.4 Da for βV-tubulin, 49 880.6 for α6-tubulin, and 50 138.4 for Kα1-tubulin.

valine to tyrosine mutation on βI-tubulin, also at position 60, has been recently selected (*29*). These findings indicate that this domain is effectively involved in lateral interactions between protofilaments. Noticeably, two hot spots of sequence divergence in β-tubulins are located in the H1−S2 and H10−S9 loops (Figures 1 and 9). As a result, the topology of these loops could be modified and contribute to the microtubule-destabilizing properties of βIII- and βV-tubulin. βV-tubulin has an additional sequence divergence in the H1−S2 loop, with a serine residue instead of an alanine residue at position 54 (Figure 1), and we speculate that human βV-tubulin has a microtubule-destabilizing potency equivalent to mouse βV-tubulin.

We and others have reported that increased expression of βIII-tubulin in cancer cells is correlated with a decreased sensitivity to Taxol, and a similar trend has been observed in patients with tumors that were poorly responsive to Taxol-based treatments (*10*). Because of the similarities between βV- and βIII-tubulin, it is conceivable that expression levels of βV-tubulin would also alter the sensitivity of cancer cells to drugs targeting microtubules. One peculiar phenotype of some cancer cells displaying decreased sensitivity to Taxol is their requirement for Taxol to sustain normal growth (*10*). It was recently reported that, when overexpression of HA-tagged mouse βV-tubulin reached 50% of the total β-tubulin in a CHO cell clone, microtubule content decreased and cell growth was dependent upon Taxol (*11*). Another clone expressed only 15−20% βV-tubulin and was slightly resistant to but not dependent upon Taxol (*11*). In the present study, the major difference between the tubulin isotype profile in A549 and Hey cells is their opposite, relative levels of βIII- and βV-tubulin. We compared the sensitivity of A549 and Hey cells to Taxol or vinblastine, and no significant difference in sensitivity to Taxol was observed (0.7 and 0.6 nM, respectively), whereas Hey cells were 2−3-fold more sensitive to vinblastine than A549 cells (0.4 and 1.2 nM, respectively). Cells, including ovarian cancer cells, that are resistant to but not dependent upon Taxol and contain a mutated βI-tubulin can also be hypersensitive to vinblastine (*10*). The fact that Hey cells were not less sensitive to Taxol despite a higher expression of βV-tubulin could result from the coexpression of a microtubule-associated protein or other endogenous protein that compensates for the microtubule-destabilizing effect of βV-tubulin. Alternatively, sequence variations among tubulin isotypes that are located in the Taxol-binding pocket may affect their affinity for Taxol. Interestingly, βIII- and mouse βV-tubulin have an alanine residue rather than the serine residue found in human βV- and βI-tubulin at position 277 (Figure 1). This residue is

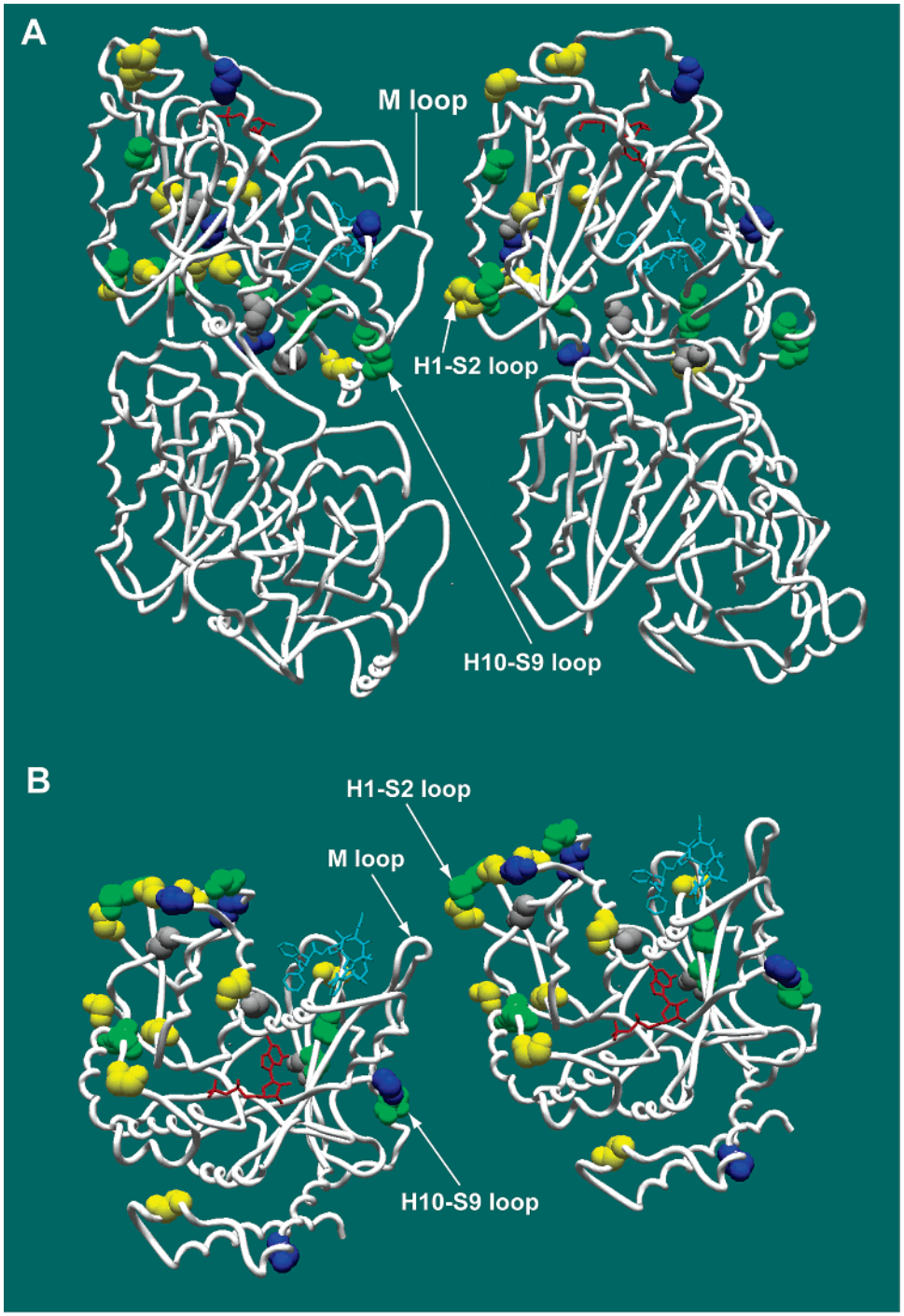

FIGURE 9: Localization of human βV-tubulin sequence divergences from human βI, βII, and βIV-tubulin on a tubulin tertiary structure model. (A) Two tubulin α/β heterodimers in adjacent microtubule protofilaments are displayed with β-tubulin at the top and viewed from the outside of the microtubule. β-tubulin is labeled with GDP in red and Taxol in light blue. Note that GTP in α-tubulin is not represented for clarity and that the α-tubulin H1−S2 loop is absent because it was not resolved in this refined tubulin dimer structure model (*25*). (B) Two adjacent β-tubulins are presented from the top. The H1−S2 loop is toward the lumen of the microtubule. Backbone atoms of divergent amino acid residues are represented in yellow (βV-tubulin), green (βV- and βIII-tubulins), dark blue (βV- and βVI-tubulins), and gray (βV-, βIII-, and βVI-tubulins). The orientation of tubulin structures in adjacent protofilaments was based on published refined microtubule models (*26*, *27*).

between threonine 276 and arginine 278, two residues located on the M loop that are part of the Taxol-binding pocket (*25*). The significance of the serine 277 residue for the structure of tubulin and for Taxol binding is suggested by the following information: (1) this residue is conserved between human α- and β-tubulins except in βIII- and βVI-tubulin; (2) it is replaced by an alanine residue in the unique β-tubulin of *Saccharomyces cerevisiae*, which does not bind Taxol (*30*); and (3) it is mutated to an arginine residue in βIII-tubulin isolated from a Taxol-resistant prostate cancer cell line (*31*). Therefore, human βV-tubulin, which conserves a serine at position 277, may bind Taxol with a higher affinity than mouse βV- or βIII-tubulin yet still maintain microtubule-destabilizing properties.

The absence of a correlation between βIII-tubulin mRNA content of human ovarian carcinoma xenografts and Taxol

sensitivity has been described (*32*), whereas such a relationship in epithelial ovarian cancer cells isolated from ascites obtained directly from patients has been observed (*16*). These discrepancies may be related to differences in starting material or in experimental design but also in βV-tubulin expression. The present study on human βV-tubulin at the protein level, the recently described destabilizing properties of mouse βV-tubulin (*11*), and the apparent complementary pattern of expression of βIII- and βV-tubulin suggest that the expression of both isotypes should be evaluated in the context of cancer cell sensitivity to drugs targeting the microtubule/tubulin system. Such extensive analysis would assess more precisely if tubulin isotype expression profiling is a clinically relevant and useful parameter for stratifying patients with cancer before initial cycles of chemotherapy and in the treatment of recurrent disease.

ACKNOWLEDGMENT

We thank Dr. Nelly Auersperg for access to the Canadian Ovarian Tissue Bank.

REFERENCES

1. Wilson, L., Panda, D., and Jordan, M. A. (1999) Modulation of microtubule dynamics by drugs: A paradigm for the actions of cellular regulators, *Cell Struct. Funct. 24*, 329−335.
2. Ludueña, R. F. (1998) Multiple forms of tubulin: Different gene products and covalent modifications, *Int. Rev. Cytol. 178*, 207−275.
3. Katsetos, C. D., Herman, M. M., and Mork, S. J. (2003) Class III β-tubulin in human development and cancer, *Cell Motil. Cytoskeleton 55*, 77−96.
4. Sullivan, K. F., Havercroft, J. C., Machlin, P. S., and Cleveland, D. W. (1986) Sequence and expression of the chicken β5- and β4-tubulin genes define a pair of divergent β-tubulins with complementary patterns of expression, *Mol. Cell. Biol. 6*, 4409−4418.
5. Banerjee, A., Roach, M. C., Trcka, P., and Ludueña, R. F. (1990) Increased microtubule assembly in bovine brain tubulin lacking the type III isotype of β-tubulin, *J. Biol. Chem. 265*, 1794−1799.
6. Panda, D., Miller, H. P., Banerjee, A., Ludueña, R. F., and Wilson, L. (1994) Microtubule dynamics *in vitro* are regulated by the tubulin isotype composition, *Proc. Natl. Acad. Sci. U.S.A. 91*, 11358−11362.
7. Derry, W. B., Wilson, L., Khan, I. A., Ludueña, R. F., and Jordan, M. A. (1997) Taxol differentially modulates the dynamics of microtubules assembled from unfractionated and purified β-tubulin isotypes, *Biochemistry 36*, 3554−3562.
8. Hari, M., Yang, H., Zeng, C., Canizales, M., and Cabral, F. (2003) Expression of class III β-tubulin reduces microtubule assembly and confers resistance to paclitaxel, *Cell Motil. Cytoskeleton 56*, 45−56.
9. Kamath, K., Wilson, L., Cabral, F., and Jordan, M. A. (2005) βIII-tubulin induces paclitaxel resistance in association with reduced effects on microtubule dynamic instability, *J. Biol. Chem. 280*, 12902−12907.
10. Orr, G. A., Verdier-Pinard, P., McDaid, H., and Horwitz, S. B. (2003) Mechanisms of Taxol resistance related to microtubules, *Oncogene 22*, 7280−7295.
11. Bhattacharya, R., and Cabral, F. (2004) A ubiquitous β-tubulin disrupts microtubule assembly and inhibits cell proliferation, *Mol. Biol. Cell 15*, 3123−3131.
12. Strausberg, R. L., Feingold, E. A., Grouse, L. H., Derge, J. G., Klausner, R. D., Collins, F. S., Wagner, L., Shenmen, C. M., Schuler, G. D., Altschul, S. F., Zeeberg, B., Buetow, K. H., Schaefer, C. F., Bhat, N. K., Hopkins, R. F., Jordan, H., Moore, T., Max, S. I., Wang, J., Hsieh, F., Diatchenko, L., Marusina, K., Farmer, A. A., Rubin, G. M., Hong, L., Stapleton, M., Soares, M. B., Bonaldo, M. F., Casavant, T. L., Scheetz, T. E., Brownstein, M. J., Usdin, T. B., Toshiyuki, S., Carninci, P., Prange, C., Raha, S. S., Loquellano, N. A., Peters, G. J., Abramson, R. D., Mullahy, S. J., Bosak, S. A., McEwan, P. J., McKernan, K. J., Malek, J. A., Gunaratne, P. H., Richards, S., Worley, K. C., Hale, S., Garcia, A. M., Gay, L. J., Hulyk, S. W., Villalon, D. K., Muzny, D. M., Sodergren, E. J., Lu, X., Gibbs, R. A., Fahey, J., Helton, E., Ketteman, M., Madan, A., Rodrigues, S., Sanchez, A., Whiting, M., Young, A. C., Shevchenko, Y., Bouffard, G. G., Blakesley, R. W., Touchman, J. W., Green, E. D., Dickson, M. C., Rodriguez, A. C., Grimwood, J., Schmutz, J., Myers, R. M., Butterfield, Y. S., Krzywinski, M. I., Skalska, U., Smailus, D. E., Schnerch, A., Schein, J. E., Jones, S. J., and Marra, M. A. (2002) Generation and initial analysis of more than 15,000 full-length human and mouse cDNA sequences, *Proc. Natl. Acad. Sci. U.S.A. 99*, 16899−16903.
13. Ota, T., Suzuki, Y., Nishikawa, T., Otsuki, T., Sugiyama, T., Irie, R., Wakamatsu, A., Hayashi, K., Sato, H., Nagai, K., Kimura, K., Makita, H., Sekine, M., Obayashi, M., Nishi, T., Shibahara, T., Tanaka, T., Ishii, S., Yamamoto, J., Saito, K., Kawai, Y., Isono, Y., Nakamura, Y., Nagahari, K., Murakami, K., Yasuda, T., Iwayanagi, T., Wagatsuma, M., Shiratori, A., Sudo, H., Hosoiri, T., Kaku, Y., Kodaira, H., Kondo, H., Sugawara, M., Takahashi, M., Kanda, K., Yokoi, T., Furuya, T., Kikkawa, E., Omura, Y., Abe, K., Kamihara, K., Katsuta, N., Sato, K., Tanikawa, M., Yamazaki, M., Ninomiya, K., Ishibashi, T., Yamashita, H., Murakawa, K., Fujimori, K., Tanai, H., Kimata, M., Watanabe, M., Hiraoka, S., Chiba, Y., Ishida, S., Ono, Y., Takiguchi, S., Watanabe, S., Yosida, M., Hotuta, T., Kusano, J., Kanehori, K., Takahashi-Fujii, A., Hara, H., Tanase, T. O., Nomura, Y., Togiya, S., Komai, F., Hara, R., Takeuchi, K., Arita, M., Imose, N., Musashino, K., Yuuki, H., Oshima, A., Sasaki, N., Aotsuka, S., Yoshikawa, Y., Matsunawa, H., Ichihara, T., Shiohata, N., Sano, S., Moriya, S., Momiyama, H., Satoh, N., Takami, S., Terashima, Y., Suzuki, O., Nakagawa, S., Senoh, A., Mizoguchi, H., Goto, Y., Shimizu, F., Wakebe, H., Hishigaki, H., Watanabe, T., Sugiyama, A., Takemoto, M., Kawakami, B., Watanabe, K., Kumagai, A., Itakura, S., Fukuzumi, Y., Fujimori, Y., Komiyama, M., Tashiro, H., Tanigami, A., Fujiwara, T., Ono, T., Yamada, K., Fujii, Y., Ozaki, K., Hirao, M., Ohmori, Y., Kawabata, A., Hikiji, T., Kobatake, N., Inagaki, H., Ikema, Y., Okamoto, S., Okitani, R., Kawakami, T., Noguchi, S., Itoh, T., Shigeta, K., Senba, T., Matsumura, K., Nakajima, Y., Mizuno, T., Morinaga, M., Sasaki, M., Togashi, T., Oyama, M., Hata, H., Komatsu, T., Mizushima-Sugano, J., Satoh, T., Shirai, Y., Takahashi, Y., Nakagawa, K., Okumura, K., Nagase, T., Nomura, N., Kikuchi, H., Masuho, Y., Yamashita, R., Nakai, K., Yada, T., Ohara, O., Isogai, T., and Sugano, S. (2004) Complete sequencing and characterization of 21,243 full-length human cDNAs, *Nat. Genet. 36*, 40−45.
14. Jai-nhuknan, J., and Cassady, C. J. (1998) Negative ion postsource decay time-of-flight mass spectrometry of peptides containing acidic amino acid residues, *Anal. Chem. 70*, 5122−5128.
15. Rao, S., Aberg, F., Nieves, E., Horwitz, S. B., and Orr, G. A. (2001) Identification by mass spectrometry of a new α-tubulin isotype expressed in human breast and lung carcinoma cell lines, *Biochemistry 40*, 2096−2103.
16. Kavallaris, M., Kuo, D. Y., Burkhart, C. A., Regl, D. L., Norris, M. D., Haber, M., and Horwitz, S. B. (1997) Taxol-resistant epithelial ovarian tumors are associated with altered expression of specific β-tubulin isotypes, *J. Clin. Invest. 100*, 1282−1293.
17. Verdier-Pinard, P., Wang, F., Burd, B., Angeletti, R. H., Horwitz, S. B., and Orr, G. A. (2003) Direct analysis of tubulin expression in cancer cell lines by electrospray ionization mass spectrometry, *Biochemistry 42*, 12019−12027.
18. Verdier-Pinard, P., Wang, F., Martello, L., Burd, B., Orr, G. A., and Horwitz, S. B. (2003) Analysis of tubulin isotypes and mutations from taxol-resistant cells by combined isoelectrofocusing and mass spectrometry, *Biochemistry 42*, 5349−5357.
19. Martello, L. A., Verdier-Pinard, P., Shen, H. J., He, L., Torres, K., Orr, G. A., and Horwitz, S. B. (2003) Elevated levels of microtubule destabilizing factors in a Taxol-resistant/dependent A549 cell line with an α-tubulin mutation, *Cancer Res. 63*, 1207−1213.
20. Ong, S. E., Blagoev, B., Kratchmarova, I., Kristensen, D. B., Steen, H., Pandey, A., and Mann, M. (2002) Stable isotope labeling by amino acids in cell culture, SILAC, as a simple and accurate approach to expression proteomics, *Mol. Cell Proteomics 1*, 376−386.
21. Ahmad, S., Singh, B., and Gupta, R. S. (1991) Nucleotide sequences of three different isoforms of β-tubulin cDNA from Chinese hamster ovary cells, *Biochim. Biophys. Acta 1090*, 252−254.

22. Roby, K. F., Taylor, C. C., Sweetwood, J. P., Cheng, Y., Pace, J. L., Tawfik, O., Persons, D. L., Smith, P. G., and Terranova, P. F. (2000) Development of a syngeneic mouse model for events related to ovarian cancer, *Carcinogenesis 21*, 585−591.
23. Regnard, C., Desbruyeres, E., Denoulet, P., and Edde, B. (1999) Tubulin polyglutamylase: Isozymic variants and regulation during the cell cycle in HeLa cells, *J. Cell Sci. 112*, 4281−4289.
24. Sawada, T., and Cabral, F. (1989) Expression and function of β-tubulin isotypes in Chinese hamster ovary cells, *J. Biol. Chem. 264*, 3013−3020.
25. Lowe, J., Li, H., Downing, K. H., and Nogales, E. (2001) Refined structure of $\alpha\beta$-tubulin at 3.5 Å resolution, *J. Mol. Biol. 313*, 1045−1057.
26. Meurer-Grob, P., Kasparian, J., and Wade, R. H. (2001) Microtubule structure at improved resolution, *Biochemistry 40*, 8000−8008.
27. Li, H., DeRosier, D. J., Nicholson, W. V., Nogales, E., and Downing, K. H. (2002) Microtubule structure at 8 Å resolution, *Structure 10*, 1317−1328.
28. Wang, Y., Veeraraghavan, S., and Cabral, F. (2004) Intra-allelic suppression of a mutation that stabilizes microtubules and confers resistance to colcemid, *Biochemistry 43*, 8965−8973.
29. Yang, C.-P. H., Verdier-Pinard. P., Wang, F., Lippaine-Horvath, E., He, L., Li, D., Hofle, G., Ojima, I., Orr, G. A., and Horwitz S. B. (2005) A highly epothilone B-resistant A549 cell line with mutations in β-tubulin that confer drug dependence, *Mol. Cancer Ther. 4*, 987−995.
30. Bode, C. J., Gupta, M. L., Jr., Reiff, E. A., Suprenant, K. A., Georg, G. I., and Himes, R. H. (2002) Epothilone and paclitaxel: Unexpected differences in promoting the assembly and stabilization of yeast microtubules, *Biochemistry 41*, 3870−3874.
31. Ranganathan, S., Dexter, D. W., Benetatos, C. A., and Hudes, G. R. (1998) Cloning and sequencing of human βIII-tubulin cDNA: Induction of βIII isotype in human prostate carcinoma cells by acute exposure to antimicrotubule agents, *Biochim. Biophys. Acta 1395*, 237−245.
32. Nicoletti, M. I., Valoti, G., Giannakakou, P., Zhan, Z., Kim, J. H., Lucchini, V., Landoni, F., Mayo, J. G., Giavazzi, R., and Fojo, T. (2001) Expression of β-tubulin isotypes in human ovarian carcinoma xenografts and in a sub-panel of human cancer cell lines from the NCI-Anticancer Drug Screen: Correlation with sensitivity to microtubule active agents, *Clin. Cancer Res. 7*, 2912−2922.

BI051004P